Nucleation on active centers in confined volumes

Zdeněk Kožíšek,[1,a)] Masamichi Hikosaka,[2] Kiyoka Okada,[2] and Pavel Demo[1]
[1]*Institute of Physics, Academy of Sciences of the Czech Republic, Cukrovarnická 10, 162 00 Praha 6, Czech Republic*
[2]*Faculty of Integrated Arts and Sciences, Hiroshima University, 1-7-1 Kagamiyama, Higashi Hiroshima 739-8521, Japan*

(Received 22 December 2011; accepted 9 April 2012; published online 26 April 2012)

Kinetic equations describing nucleation on active centers are solved numerically to determine the number of supercritical nuclei, nucleation rate, and the number density of nuclei for formation both of droplets from vapor and also crystalline phase from vapor, solution, and melt. Our approach follows standard nucleation model, when the exhaustion of active centers is taken into account via the boundary condition, and thus no additional equation (expressing exhaustion of active centers) is needed. Moreover, we have included into our model lowering of supersaturation of a mother phase as a consequence of the phase transition process within a confined volume. It is shown that the standard model of nucleation on active centers (Avrami approach) gives faster exhaustion of active centers as compared with our model in all systems under consideration. Nucleation rate (in difference to standard approach based on Avrami model) is equal to the time derivative of the total number of nuclei and reaches some maximum with time. At lower nucleation barrier (corresponding to higher initial supersaturation or lower wetting angle of nucleus on the surface of active center) the exhaustion of active centers is faster. Decrease in supersaturation of the mother phase is faster at higher number of active centers. © *2012 American Institute of Physics*. [http://dx.doi.org/10.1063/1.4705436]

I. INTRODUCTION

Phase transition is initiated within original metastable phase by nucleation of small regions of the new phase.[1] Due to fluctuations within supersaturated (or supercooled) mother phase the clusters of various sizes are formed. Small clusters have tendency to disappear but after reaching some critical size they grow up to macroscopic sizes. Supercritical clusters are called nuclei. At the critical size the free energy of the formation of a cluster reaches the maximum called the nucleation barrier. This energy barrier depends on the imposed thermodynamic conditions.

Homogeneous nucleation corresponds to the case when any molecule serves as a nucleation site with subsequent cluster formation, while heterogeneous nucleation is initialized on the heterogeneities (e.g., foreign particles, walls of the vessel, structure defects, ions). Nucleation on active centers is a special case of heterogeneous nucleation, when the clusters are formed on the energetically preferred sites.[2] In some cases it is difficult to determine which heterogeneities serve as active centers, e.g., in atmosphere the dusty particles, volcanic, and industry emissions, ions, etc. represent possible active centers, on which the formation of nuclei preferentially occurs. Additives can also influence the transport of molecules to the phase interface or initialize nucleation (active centers). In many experiments the active centers may be controlled. Kumomi and Shi[3] initialized solid-phase crystallization of amorphous Si thin films from the vapor phase at the artificially prepared nucleation sites. Fokin *et al.*[4] observed the number of crystals formed on the polished surface of cordierite glass on two different kind of the active surface sites (active centers). So called nucleation agent (forming nucleation centers) was added to increase the rate of formation of the crystal nuclei of folded chain polyethylene.[5–7] McClurg[8] identified criteria for the ideal foam nucleating agents to produce desirable foams with a large number density and, simultaneously, with the narrow size distribution of bubbles.

The standard approach to nucleation on active centers[2,9] is based on Avrami model,[10,11] which determines the total number of supercritical nuclei, Z, from the following equation:

$$\frac{dZ(t)}{dt} = J_A[N_{AC} - Z(t)], \tag{1}$$

where N_{AC} is the number of active centers and J_A is the nucleation rate per active center. At time t only $[N_{AC} - Z]$ centers are unoccupied to serve as the nucleation sites for new nuclei. If time delay (sometimes called time lag or transient time) of nucleation is very short, one can approximate nucleation rate by its stationary value, J_A^S, to get

$$Z(t) = N_{AC}\left[1 - \exp(-J_A^S t)\right]. \tag{2}$$

It is evident that at $t \to \infty$ the total number of supercritical nuclei corresponds to the number of active centers N_{AC}.

If we consider nonstationary nucleation, we get[2]

$$Z(t) = N_{AC}\left\{1 - \exp\left[-\int_0^t J_A(t')dt'\right]\right\}, \tag{3}$$

with unknown nucleation rate $J_A(t)$. Various analytical approaches exist to obtain the expression for nonstationary

a)Electronic mail: kozisek@fzu.cz. URL: http://www.fzu.cz/~kozisek/.

nucleation rate, e.g., Kashchiev[2] derived widely used analytical formula

$$J_A(t) = J_A^S \left[1 + 2 \sum_{i=1}^{\infty} (-1)^i \exp(-i^2 t/\tau) \right], \tag{4}$$

where

$$\tau = 4/(\pi^3 z^2 k_{i^*}^+) \tag{5}$$

denotes the time delay of nucleation, z is so called Zeldovich factor, and $k_{i^*}^+$ is the attachment frequency of "the building units of a new phase" (atoms, molecules, or repeating units of polymer chain) to the critical cluster (for details see Sec. II.). Above equations determine the standard model of nucleation on active centers.[2]

Nucleation rate, i.e., the number of nuclei of the critical size formed in unit volume (on unit surface) per unit time, is usually determined as the time derivative of the number of supercritical nuclei. Problem is that $J_A(t)$ is determined from the kinetic equations under the condition that the number of active centers, on which nuclei can be formed, does not change with time. On the other hand it is evident that the number of active centers decreases with time as the exhaustion of active centers occurs.

We have already suggested,[12] and applied to various systems,[13–17] the model of nucleation on active centers based on the standard nucleation kinetics which does not need to include the governing Eq. (1).

In this work, we deal with nucleation on active centers for the crystal nucleation from supersaturated vapor, solution, supercooled melt, and also for the formation of droplets in supersaturated vapor in a confined volume. Contrary to previous works a decrease in supersaturation of the mother phase, due to the transformation of molecules from the mother to the new phase, is included to our model of nucleation on active centers. Numerical solution of kinetic equations determines the number density of nuclei, nucleation rate, and the total number of nuclei by contrast to the standard model of nucleation on active centers [based on Eq. (1)], which gives only the total number of supercritical nuclei. Comparison of the number density of nuclei and nucleation rate with the experimental data help us to better understand the phase transition on active centers.

II. MODEL

The transient frequencies of attachment, k_i^+, and detachment, k_i^-, depend on the system under consideration. Hereafter, we will shortly summarize the basic kinetic equations. Formation of nuclei within standard nucleation theory, when the addition of "growth units" (atoms, molecules, or repeating unit of polymer chain) plays a dominant role and the coalescence of nuclei is neglected, is governed by[1,18–20]

$$\frac{dF_i(t)}{dt} = k_{i-1}^+ F_{i-1} - [k_i^+ + k_i^-] F_i + k_{i+1}^- F_{i+1} = J_{i-1} - J_i, \tag{6}$$

where

$$J_i(t) = k_i^+ F_i - k_{i+1}^- F_{i+1} \tag{7}$$

is the rate of formation of i-sized nuclei and $F_i(t)$ denotes the number density of nuclei consisting of i molecules in a unit volume at time t. The total number of nuclei greater than a certain nucleus size m is determined as follows:

$$Z_m(t) = \sum_{i>m} F_i(t) = \int_0^t J_m(t')dt'. \tag{8}$$

Experimental values of Z_m usually correspond to some detectable size, which determines m. Eq. (3) gives the approximate analytical solution for the number of supercritical nuclei, i.e., for $m = i^*$. We can also determine the analytical approach to Z_m for $m > i^*$ using analytical solution of Shneidman[21] for the cluster flux at supercritical size [instead of J_A in Eq. (3)].

Detachment frequency is determined from the local thermodynamic equilibrium (when $J_i = 0$) to be

$$k_i^+ F_i^0 = k_{i+1}^- F_{i+1}^0, \tag{9}$$

where the equilibrium number density of nuclei within the self consistent classical model can be expressed as[22,23]

$$F_i^0 = F_1 \exp\left(\frac{W_1}{k_B T}\right) \exp\left(-\frac{W_i}{k_B T}\right). \tag{10}$$

Here, T denotes temperature, k_B is the Boltzmann constant, W_i is the work of formation of nuclei formed by i monomers, and F_1 is the number of active centers on which the formation of nuclei occurs.

At the stationary state ($J_i(t) = J^S = const.$) the rate of formation of nuclei does not change with nucleus size and time. The exact analytical formula for the stationary nucleation rate is given by[1]

$$J^S = \left(\sum_{i=1}^{\infty} \frac{1}{k_i^+ F_i^0} \right)^{-1}. \tag{11}$$

The approximate stationary nucleation rate[2]

$$J^S = z F_{i^*}^0 k_{i^*}^+ \tag{12}$$

was derived under the assumption of continuous nucleus size. Above,

$$z = \sqrt{\frac{1}{2\pi k_B T} \left(-\frac{\partial^2 W_i}{\partial i^2} \right)_{i^*}} \tag{13}$$

denotes the Zeldovich factor.

The initial and boundary conditions play important role. At initial time we suppose that no nuclei are present within considered system and the number of "monomers" (nucleation sites on which nucleation occurs) is equal to the number of active centers, i.e.,

$$F_1(t = 0) = N_{AC}, \tag{14}$$

$$F_i(t = 0) = 0 \quad \text{for i} > 1. \tag{15}$$

As F_i stands for the number density of i-sized nuclei thus F_1 represents the number of single molecules on active centers. Adsorption of molecules on a surface is very complicated process (see, e.g., Zhou and Huang,[24] Schimka *et al.*[25]). Adsorption energy, E_A, depends on the surface substrate structure, adsorption site, etc. Dimensions of the active centers can be distinct: from atomic scale (e.g., points defects, ions) up to macroscopic sizes (e.g., nucleation agent added to the supercooled melt[5]). If we consider very small active center, the number of monomers $F_1(t = 0) = N_{AC}\exp(-E_A/k_BT)$, i.e., Eq. (14) holds for very small adsorption energies (or at high temperature T). If E_A is sufficiently large, the number of monomers is less then N_{AC}, and the size distribution of nuclei will be lowered by $\exp(-E_A/k_BT)$ factor. On the other hand on the surface with larger active center several molecules can be adsorbed. Measured number of nuclei on active centers[6,7] have shown that on one active center is formed one nucleus. For the sake of simplicity we suppose that at initial time every active center is occupied by one molecule. In a standard nucleation model it is also supposed that the number of monomers, F_1, does not change with time, i.e., $F_1(t) \gg \sum_{i>1} iF_i(t)$ and thus

$$F_1(t) = N_{AC}. \tag{16}$$

Nevertheless, as nuclei are formed on active centers, part of these centers is occupied by newly created nuclei and new nuclei can be formed only at "*unoccupied centers*." Thus, the exhaustion of the active centers can be expressed as follows:

$$F_1(t) = N_{AC} - \sum_{i>1} F_i(t). \tag{17}$$

Consequently, N_{AC} corresponds to the total number of active centers (exhausted as new nuclei are formed). Moreover we suppose a confined volume and that is why we include the following condition:

$$N_1(t) = N_T - \sum_{i>1} i\,F_i(t), \tag{18}$$

where N_1 is the number of molecules (atoms) in the supersaturated or supercooled mother phase at time t and $N_T = N_1(t = 0)$ is the total number of molecules within system. Sum in Eq. (18) represents the total number of molecules (atoms) "transferred" from the mother to the new phase.

A. Crystal nucleation from vapor

Let us consider the formation of the crystalline phase from the supersaturated vapor on the active centers located on flat substrate. Kumomi and Shi[3] studied experimentally the same type of phase transition. The attachment frequency is given by (for details see Kožíšek *et al.*[12])

$$k_i^+ = \frac{P}{\sqrt{2\pi m_1 k_B T}} A_i \exp\left(-\frac{E}{k_B T}\right), \tag{19}$$

where P is the vapor pressure, E is the mean value of the activation energy of diffusion of molecules across the phase interface, m_1 denotes the atomic mass of molecules forming the nucleus, and

$$A_i = \gamma_0 i^{2/3} \tag{20}$$

is the surface area of i-sized cluster (subcritical or supercritical) in contact with the supersaturated vapor and the geometrical factor reads:

$$\gamma_0 = 2\pi\left(\frac{3m_1}{4\pi\varrho\psi(\alpha)}\right)^{2/3}(1-\cos\alpha) \tag{21}$$

for the hemispherical nucleus. ϱ stands for the density of the crystalline phase, α is the wetting angle, and

$$\psi(\alpha) = \frac{1}{4}(1-\cos\alpha)^2(2+\cos\alpha). \tag{22}$$

The work of formation of nuclei can be expressed within capillarity approximation as

$$W_i = -i\,\Delta\mu + \beta i^{2/3}, \tag{23}$$

where $\beta = \gamma_1\sigma$, σ is interfacial energy, and

$$\gamma_1 = \sqrt[3]{36\pi\psi(\alpha)}\left(\frac{m_1}{\varrho}\right)^{2/3}. \tag{24}$$

The term $\beta i^{2/3}$ in Eq. (23) represents the surface energy of i-sized nucleus,

$$\Delta\mu = k_B T \ln S \tag{25}$$

denotes the difference in the chemical potentials of molecules between crystalline nucleus and vapor, $S = P/P_0$ is the supersaturation, and P_0 stands for the equilibrium pressure of the vapor.

For subcritical cluster sizes the work of formation of clusters increases with cluster size and thus one additional term would be taking into account. Turnbull and Fisher[26] assumed that during growth of the subcritical clusters the system passes through a configuration that is higher in energy than the original state to derive the transient frequencies in condensed systems. This term would be incorporated also for the vapor-solid phase transition and thus

$$k_i^+ = \frac{P}{\sqrt{2\pi m_1 k_B T}} A_i \exp\left(-\frac{E}{k_B T}\right)\exp\left(-\frac{q\Delta g_i}{k_B T}\right), \tag{26}$$

where $\Delta g_i = W_{i+1} - W_i$ and

$$q = 0.5[1 + \mathrm{sign}(\Delta g_i)]. \tag{27}$$

Influence of the last term in Eq. (26) on the nucleation kinetics is discussed in Sec. III for the formation of droplets from a vapor.

The work of formation of nuclei reaches maximum called nucleation barrier, which occurs at critical size

$$i^* = \left(\frac{2\beta}{3\Delta\mu}\right)^3. \tag{28}$$

B. Formation of droplets from vapor

As a second system we consider the formation of droplets from the supersaturated vapor. Active centers can be placed on a substrate (as in previous case) or within a volume of the

supersaturated vapor. In both cases the formation of nuclei is governed by the same kinetic equations. Let us consider the active centers placed within a volume of the supersaturated vapor. For the sake of simplicity, we suppose that the active centers are sufficiently large in comparison with nucleus size and thus the surface of active center can be considered as flat (otherwise it is necessary to include the consequences of the surface curvature on the work of formation of nuclei – see Cooper *et al.*[27]). F_i thus determines the number of i-sized nuclei formed in unit volume.

Work of formation of nuclei is determined by the same way as in previous case, i.e., Eqs. (23)–(24) were used with the exception that ϱ in Eq. (24) represents now the density of the liquid phase. Attachment frequency was computed from Eq. (19) and also from Eq. (26) with $E = 0$ [i.e., $\exp(-E/k_BT) = 1$ for the formation of droplets from the supersaturated vapor].

C. Crystal nucleation of supercooled polymer melt

Crystallization of polyethylene is studied for a long time due to high application potential. We considered nucleation of the folded chain crystals of polyethylene on active centers from supercooled melt, when experimental data of the total number of nuclei[5] and also the number density of nuclei[28] were obtained. In polymer systems the building units of a new phase consist of several molecules (CH_2 group for polyethylene) bounded with other building units even in the supercooled melt. Work of formation of the (3D) polyhedral form of nucleus with edges a, b, c can be expressed by Eq. (23) (for details see Kožíšek *et al.*[17]), where the difference in chemical potentials is given by

$$\Delta\mu = \frac{\Delta h_E}{N_A T_m^0}\Delta T, \tag{29}$$

$$\beta = 3\sqrt[3]{4\sigma^1\sigma_e^1\Delta\sigma^1}, \tag{30}$$

$\Delta T = T_m^0 - T$ denotes supercooling. The following material parameters were selected for polyethylene: heat of fusion $\Delta h_e = 4.11\,\mathrm{kJ/mol}$ and the equilibrium temperature $T_m^0 = 412.65\,\mathrm{K}$. Index 1 in Eq. (30) expresses that the interfacial energies are taken per one "growth unit" – for details see Kožíšek *et al.*[17] $\Delta\sigma = \sigma_{CL} + \sigma_{AC} - \sigma_{AL}$, where σ_{CL}, σ_{AC}, and σ_{AL} denote the interfacial energies between nucleus and liquid, nucleus and active center, and active center and liquid; σ is the side surface energy ($b \times c$ surface) and σ_e designates the end surface energy ($a \times b$ surface). The critical nucleus size can be expressed by[17]

$$i^* = \frac{32\sigma^1\sigma_e^1\Delta\sigma^1}{(\Delta\mu)^3}. \tag{31}$$

Attachment frequency reads

$$k_i^+ = 2l\left(\frac{k_BT}{h}\right)\exp\left(-\frac{E}{k_BT}\right)\exp\left(-\frac{q\Delta g_i}{k_BT}\right), \tag{32}$$

where h is the Planck's constant and l designates the number of monomers on the $b \times c$ surface.

D. Crystal nucleation from solution

As the last system, the crystal nucleation on active centers from solution, when the active centers are added to a volume of the supersaturated solution, were considered. For the sake of simplicity we suppose flat surface of active center and also assume that nucleation is the slowest process, and thus the solution is homogeneous (constant concentration within the volume).

The work of formation of nuclei is determined by Eqs. (23)–(25) with supersaturation $S = C/C^0$, where C is the actual concentration in solution and C^0 denotes the equilibrium concentration of the component that forms the nucleus.

The attachment frequency is expressed in the standard way,[2]

$$k_i^+ = N_S C A_i\left(\frac{k_BT}{h}\right)\exp\left(-\frac{E}{k_BT}\right)\exp\left(-\frac{q\Delta g_i}{k_BT}\right), \tag{33}$$

where N_S is the number density of nucleation sites on the nucleus surface.

III. RESULTS AND DISCUSSION

We have numerically solved Eq. (6) to determine the number of supercritical nuclei, nucleation rate, and the number density of nuclei formed on the active centers for vapor-solid, melt-solid, solution-solid, and vapor-liquid phase transition.

Volume size plays important role in the phase transition processes[29–33] but these effects are out of scope of this work.

A. Crystal nucleation from vapor

At the numerical computations we have used the same input parameters as in our previous work,[12] i.e., $N_{AC} = 4 \times 10^8\,\mathrm{m}^{-2}$, $P = 2\,\mathrm{Torr}$ (266.644 Pa), $P_0 = 1.2\,\mathrm{Torr}$ (159.9864 Pa), $T = 1073\,\mathrm{K}$, $\varrho = 3512.56\,\mathrm{kg\,m}^{-3}$, $m_1 = 2 \times 10^{-26}\,\mathrm{kg}$, $\sigma = 0.25\,\mathrm{J\,m}^{-2}$, $\alpha = 90^\circ$, and $E = 3.19 \times 10^{-19}\,\mathrm{J}$. The attachment frequency was computed by the standard way from Eq. (19).

We have compared the total number of nuclei greater than the critical size ($i^* = 19.47$) computed by the numerical solution of Eq. (6) using the boundary condition (17) [solid line in Fig. 1] with the analytical solution [see Eqs. (3)–(5), dashed line in Fig. 1]. Moreover we have also used in the numerical computation the boundary condition (16) instead of (17) to determine the number of supercritical nuclei in the standard model (dotted line in Fig. 1). At a very short time, when the exhaustion of active centers is relatively small, the analytical solution [dashed line, Eqs. (3)–(5)] is close to the numerical solution (dotted line) using Eq. (16) as boundary condition instead of Eq. (17) – see Fig. 1. The number of supercritical nuclei reaches the number of active centers N_{AC} at sufficiently long time, but Kashchiev solution [see Eqs. (3)–(5), dotted line] reaches this value faster in comparison with our model (solid line). The number of the supercritical clusters per active center, Z_{i^*}/N_{AC}, does not change with the number of active centers, N_{AC}.

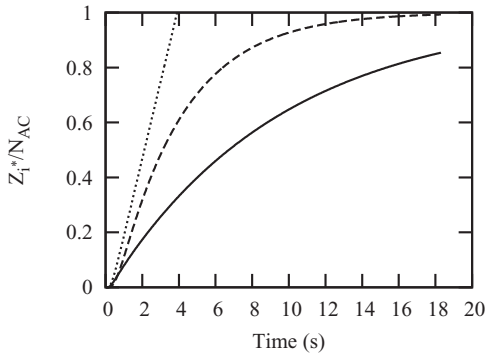

FIG. 1. The number of supercritical nuclei, Z_{i^*}, normalized by the number of active centers, N_{AC}, as a function of time for numerical solution of Eq. (6) with boundary condition (17) [solid line], respectively, (16) [dotted line], and analytical solution [Eqs. (3)–(5), dashed line].

Nucleation rate at the critical size, J_{i^*}, is the time derivative of the number of supercritical nuclei Z_{i^*} – see Eq. (8). The analytical approach to Z [see Eq. (3)] is based on the nucleation rate per active center, J_A, derived for the system with constant number of active centers [see Eq. (16)], and thus differs from the time derivative of Z. The analytical solution of the nucleation rate [see Eq. (4), dashed line in Fig. 2] is close to the numerical solution of Eq. (6) at constant number of active centers [see Eq. (16), dotted line]. However, the exhaustion of the active centers occurs as nuclei are formed [see Eq. (17)]. As a consequence, a maximum in the time dependence of the nucleation rate, determined by the numerical solution of Eq. (6), appears – see solid line in Fig. 2. The numerical solution of the nucleation rate, taking into account the exhaustion of active centers [using Eq. (17)], reaches some maximum with time – see solid line in Fig. 2. At shorter time, when the exhaustion of active centers is low, all dependencies (solid, dashed, and dotted lines) have similar progress. The stationary nucleation rate, J^S, was determined from Eq. (11) at $t = 0$.

A decrease in the supersaturation of vapor was negligible for forementioned values of input parameters. From this reason we have increased the total number of active centers to

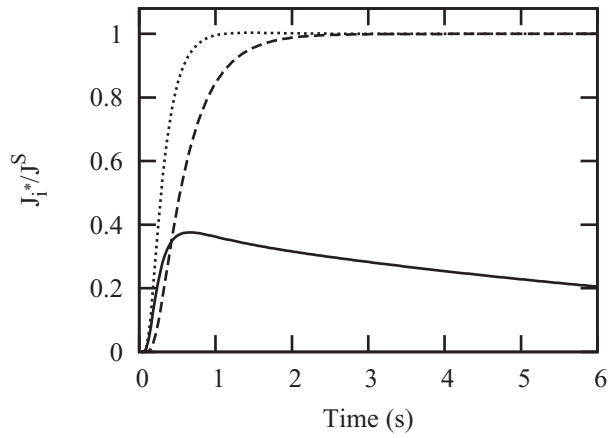

FIG. 2. Nucleation rate at the critical size, J_{i^*}, normalized by the stationary nucleation rate, J^S, as a function of time for numerical solution of Eq. (6) with boundary condition (17) [solid line], respectively, (16) [dotted line], and analytical solution [Eqs. (4)–(5), dashed line].

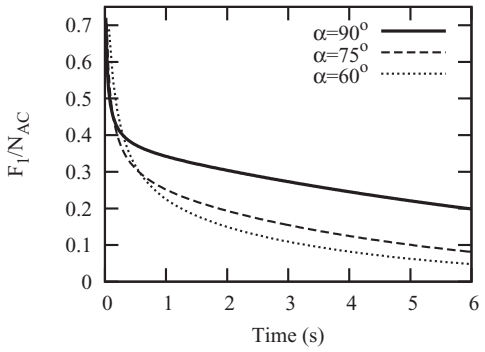

FIG. 3. The number of unoccupied active centers, F_1, normalized by the total number of active centers, N_{AC}, as a function of time for wetting angles $\alpha = 90^\circ$ (solid line), 75° (dashed line), and 60° (dotted line).

$N_{AC} = 10^{15}\,\mathrm{m}^{-2}$. The number of monomers (active centers, where no nucleus is formed), F_1, decreases with time (see Fig. 3) due to the exhaustion of the active centers. The slowest decrease of F_1 occurs at $\alpha = 90^\circ$ (solid line), faster decrease at $\alpha = 75^\circ$ (dashed line), and at $\alpha = 60^\circ$ (dotted line). The exhaustion of active centers (i.e., decrease in F_1) is faster as wetting angle, α, decreases (i.e., the nucleation barrier decreases). The nucleation barrier decreases with decreasing wetting angle α and the exhaustion of active centers (i.e., the decrease in F_1) is faster.

At $N_{AC} = 10^{15}\,\mathrm{m}^{-2}$ a decrease in the supersaturation of vapor has appeared (Fig. 4). As wetting angle α decreases, the nucleation barrier is lower and thus one could expect faster decrease in the supersaturation of vapor. Actually, the decrease in the supersaturation has just opposite behavior: at $\alpha = 90^\circ$ is faster (solid line in Fig. 4) than at $\alpha = 75^\circ$ (dashed line in Fig. 4), and $\alpha = 60^\circ$ (dotted line in Fig. 4).

Decrease in supersaturation of vapor (see Fig. 4) can be explained from the number density of clusters – see Fig. 5. The number of nuclei near the critical size at time $t = 6$ s decreases with cluster size. A decrease of F is faster at $\alpha = 90^\circ$ (solid line in Fig. 5) in comparison with $\alpha = 75^\circ$ (dashed line) and $\alpha = 60^\circ$ (dotted line). At smaller cluster sizes ($i \leq 10$), the number of clusters at $\alpha = 90^\circ$ is higher than at $\alpha = 75^\circ$ and 60° (the exhaustion increases with decrease of the wetting angle α). Decrease in supersaturation (Fig. 4) is governed by Eq. (18). The subcritical clusters contribute to a decrease in the number of molecules in vapor, N_1, and thus decrease

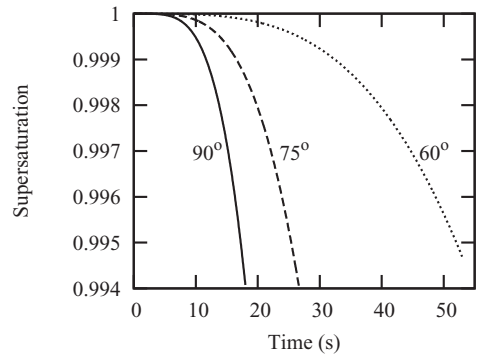

FIG. 4. Supersaturation of vapor as a function of time for $\alpha = 90^\circ$ (solid line), 75° (dashed line), and 60° (dotted line).

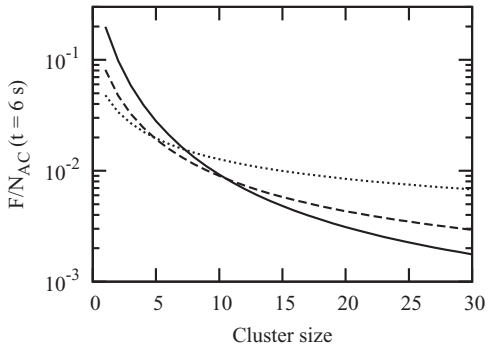

FIG. 5. The number density of nuclei, F, normalized by the total number of active centers, N_{AC}, as a function of cluster size at $\alpha = 90^\circ$ (solid line), 75° (dashed line), and 60° (dotted line) at time $t = 6$ s.

in the supersaturation is faster – see Fig. 4. The lowering in supersaturation as a function of wetting angle α could differ if we consider the equilibrium size distribution of nuclei at $t = 0$. The influence of the initial size distribution of nuclei on homogeneous nucleation kinetics in a closed system was studied in our previous work.[34] At the supercritical sizes of nuclei, the number of nuclei at the same time $t = 6$ s is higher at lower α as the nucleation barrier decreases.

Experimental data on the total number of nuclei correspond to a certain detectable size, which is closely connected to the used experimental method. However, the critical size depends on the thermodynamic parameters (e.g., wetting angle, temperature, supersaturation, interfacial energy). That is why we selected the same size $m = 1000$ and computed Z_m [see Eq. (8)] for various α – see Fig. 6. Z_{1000} approaches the total number of active centers, N_{AC}, as time increases. At the wetting angle $\alpha = 90^\circ$ (solid line in Fig. 6) the increase in Z_{1000} is lower (lower nucleation rate) as compared with $\alpha = 75^\circ$ (dashed line) and 60° (dotted line). The lower wetting angle gives the lower nucleation barrier and thus the higher nucleation rate (time derivative of Z).

B. Formation of droplets from vapor

The formation of droplets on the active centers within a volume of the supersaturated ethanol vapor with the following material parameters:[35] $T = 260$ K, $\varrho = 0.8175\,\mathrm{kg\,m^{-3}}$, $P^0 = 598.36$ Pa, and $\sigma = 0.02502\,\mathrm{J\,m^{-2}}$ was selected as the second system.

The time delay of droplet nucleation from supersaturated vapor is typically very short ($\approx \mu$s) and thus the stationary nucleation is usually measured. The attachment frequency, k_i^+, in a standard model is determined by Eq. (19). If we take into account the fact that the work of formation of nuclei increases with a cluster size in the subcritical region, we get for k_i^+ Eq. (26). The stationary nucleation rate determined according to Eq. (12) gives the same values in both cases, e.g., for $S = 5$, $\alpha = 90^\circ$, $N_{AC} = 10^{15}\,\mathrm{m^{-3}}$ one gets $J^S = 8.45 \times 10^{19}\,\mathrm{m^{-3}s^{-1}}$. The last term in Eq. (26) decreases the attachment frequency at $i < i^*$ and thus the stationary nucleation rate is lower [see Eq. (11); the exact solution of the stationary nucleation rate]. If we use for k_i^+ Eq. (19) [respectively, Eq. (26)], we get for the same parameters from Eq. (11) $J^S = 8.32 \times 10^{19}\,\mathrm{m^{-3}s^{-1}}$ [respectively, $J^S = 7.30 \times 10^{19}\,\mathrm{m^{-3}s^{-1}}$]. The differences are small if we consider the inaccuracies in the measurement of the stationary nucleation rate.

The number densities, F, determined by the numerical solution of Eq. (6) (see Fig. 7) using the attachment frequency established by Eq. (26) [solid lines] and (19) [dashed lines] differ only slightly. We have compared both these approaches for $t = 0.6\,\mu$s, $1.2\,\mu$s, $2\,\mu$s, and $3\,\mu$s (Fig. 7). Both expressions [Eq. (26) or (19)] for the attachment frequency give very similar results in the number density of nuclei. In the following computations the attachment frequency was determined from Eq. (26).

The total number of the supercritical nuclei, Z_{i^*}, for $N_{AC} = 10^{15}\,\mathrm{m^{-3}}$ and the initial supersaturation $S = 5$ increases slowly at the wetting angle $\alpha = 90^\circ$, but at $\alpha = 60^\circ$ Z_{i^*} reaches N_{AC} value in a relatively short time – see Fig. 8. In both cases the increase of Z_{i^*} with time for the numerical solution of Eq. (6) is slower (solid lines) in comparison with the analytical solution [dashed lines; Eqs. (3)–(5)]. The number of supercritical nuclei reaches the total number of nuclei, N_{AC}, faster at lower nucleation barrier W^* (at $\alpha = 90^\circ$, W^* is higher than at $\alpha = 60^\circ$).

The number of active centers, F_1, on which nucleation occurs, decreases [for $N_{AC} = 10^{15}\,\mathrm{m^{-3}}$, $S(t = 0) = 5$] with

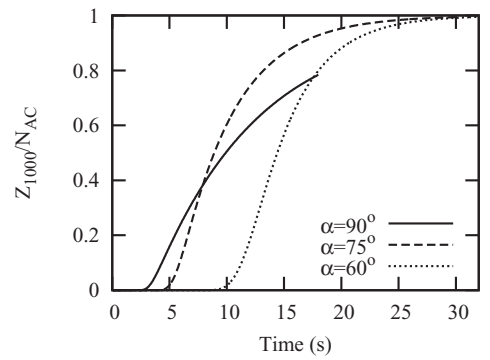

FIG. 6. Total number of nuclei per active center greater than 1000 molecules, Z_{1000}/N_{AC}, as a function of time at $\alpha = 90^\circ$ (solid line), 75° (dashed line), and 60° (dotted line).

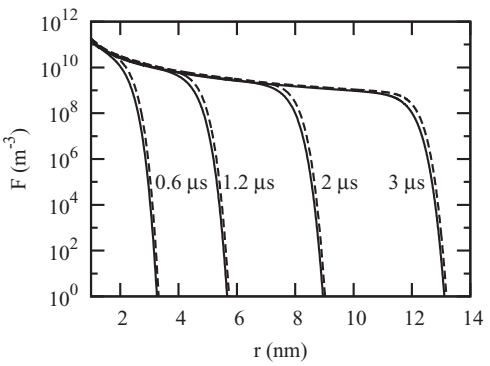

FIG. 7. Number of nuclei, F, as a function of droplet radius, r, for times $t = 0.6\,\mu$s, $1.2\,\mu$s, $2\,\mu$s, and $3\,\mu$s. The attachment frequency was determined from Eqs. (26) [solid lines] and (19) [dashed lines].

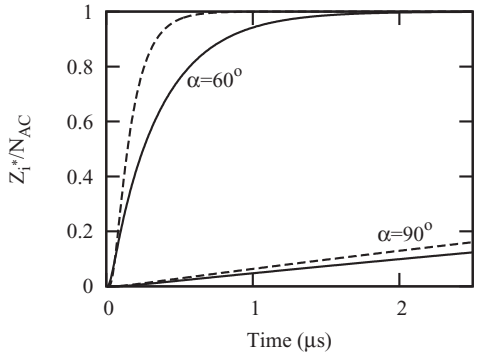

FIG. 8. The total number of supercritical nuclei per active center, Z_{i*}/N_{AC}, as a function of time at wetting angle $\alpha = 90^\circ$ and 60° for numerical (solid lines), and analytical (dashed lines) solutions.

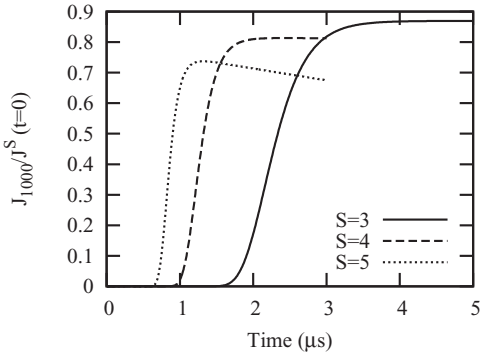

FIG. 10. Nucleation rate at nucleus size 1000, J_{1000}, normalized by the stationary nucleation rate, J^S, as a function of time at initial supersaturations $S(t = 0) = 3$ (solid line), 4 (dashed line), and 5 (dotted line).

increasing time – see Fig. 9. For the wetting angle $\alpha = 120^\circ$ (solid line) F_1/N_{AC} reaches value ≈0.88 in a short time and then the further decrease continues slowly; at $\alpha = 90^\circ$ (dashed line), and 60° (dotted line) decrease of F_1 is faster. The nucleation barrier increases with the wetting angle and thus higher exhaustion of the active centers at lower α is essential.

We have compared the nucleation rates (see Fig. 10) at the initial supersaturations $S = 3$ (solid line), 4 (dashed line), and 5 (dotted line) for the same size $i = 1000$. As the initial supersaturation increases, time delay of nucleation is shorter and the maximum of nucleation rate is lower. At lower supersaturation ($S = 3$), the nucleation barrier is higher and the decrease in the nucleation rate at longer times ($t > 3\,\mu$s) is very small (see solid line in Fig. 10).

The decrease in the supersaturation of vapor is insignificant at lower number of active centers ($N_{AC} < 10^{15}\,\mathrm{m}^{-3}$). As the total number of active centers increases ($N_{AC} > 10^{15}\,\mathrm{m}^{-3}$), the decrease in the supersaturation is higher – see Fig. 11. The influence of the increasing number of the active centers, N_{AC}, to the decrease in the supersaturation as a function of time is similar to the influence of wetting angle – see Fig. 3. However, the origin of this decrease is different: at lower wetting angle is lower nucleation barrier but the higher number of active centers (nucleation sites) does not influence the nucleation barrier. At $N_{AC} = 10^{15}$ supersaturation of vapor remains approximately unchanged (solid line), and decreases at $N_{AC} = 10^{16}$ (dashed line) and $10^{17}\,\mathrm{m}^{-3}$ (dotted line).

C. Crystal nucleation of supercooled polymer melt

We have already analysed data on the total number of supercritical nuclei of polyethylene[16] at supercooling $\Delta T = 10.4\,\mathrm{K}$ and also the number of nuclei as a function of time.[17] The following values of input parameters (used in this work for the numerical computation): $\sigma = 0.0073$, $\sigma_e = 0.00185$, and $\Delta\sigma = 0.0009\,\mathrm{J\,m}^{-2}$; $E/(k_BT) = 29.2$, and $N_{AC} = 5.8 \times 10^{16}\,\mathrm{m}^{-3}$ give the best coincidence between our model and the experimental data of the total number of supercritical nuclei and the number densities of nuclei.[17] The critical size of nucleus $i^* = 438$ is much higher than in other considered systems.

At the phase transition part of growth units is transferred from the supercooled melt to the new folded chain crystalline form of polyethylene and thus the decrease in the number of growth units in the melt occurs. This decrease does not influence the formation of nuclei as the attachment frequencies [see Eq. (32)] and also the detachment frequencies [see Eq. (9)] does not change.

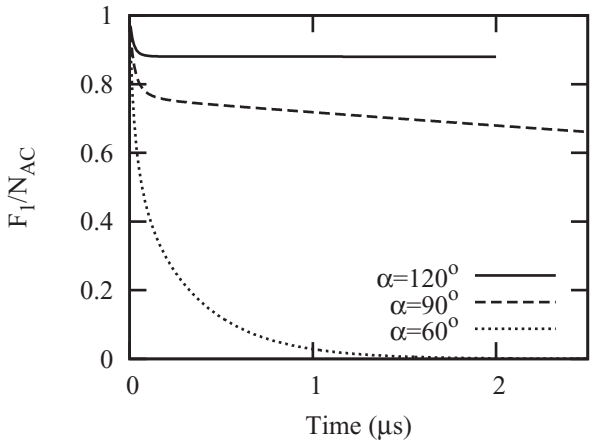

FIG. 9. Decrease of number of monomers per active center, F_1/N_{AC}, as a function of time at initial supersaturation $S(t = 0) = 5$ for wetting angles $\alpha = 120^\circ$ (solid line), 90° (dashed line), and 60° (dotted line).

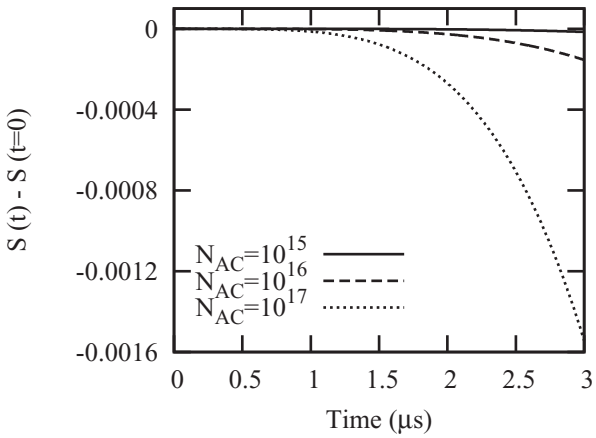

FIG. 11. Decrease in supersaturation as a function of time for $N_{AC} = 10^{15}$ (full line), 10^{16} (dashed line), and $10^{17}\,\mathrm{m}^{-3}$ (dotted line).

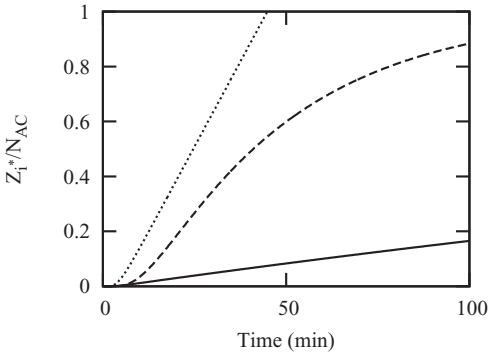

FIG. 12. The number of supercritical nuclei per active center, Z_{i^*}/N_{AC}, as a function of time. Solid and dotted lines correspond to the numerical solution of Eq. (6) with boundary condition (16) and (17), dashed line corresponds to the analytical solution [see Eqs. (3)–(5)].

The stationary nucleation rate $J^S = 2.39 \times 10^{13}\,\mathrm{m^{-3}\,s^{-1}}$ determined from the exact Eq. (11) gives rather higher value than the approximate solution (12) ($J^S = 1.57 \times 10^{13}\,\mathrm{m^{-3}\,s^{-1}}$).

We have compared the total number of supercritical nuclei Z_{i^*} (see Fig. 12), determined by the numerical solution of Eq. (6), with boundary condition (17) (solid line) and (16) (dotted line). The approximate analytical solution of the number of the supercritical nuclei [see Eqs. (3)–(5), dashed line] increases with time faster than our model gives (solid line).

In the standard model ($F_1(t) = N_{AC}$) the nucleation rate at critical size, J_{i^*}, reaches at sufficiently long time the stationary value, J^S, for the numerical solution of Eq. (6) (dotted line in Fig. 13) and also for the approximate analytical solution [see Eq. (4), dashed line]. On the other hand the dimensionless nucleation rate, J_{i^*}/J^S, determined by the numerical solution of Eq. (6) with the boundary condition (17) reaches maximum (≈0.075) and then slowly decreases with time (see Fig. 13).

The nucleation rate at $i = 450$ (solid line), 3000 (dashed line), and 30 000 (dotted line) reaches some maximum and then slowly decreases with time – see Fig. 14. The time delay of nucleation increases with nucleus size i.

The number of monomers, F_1, (i.e., the number of active centers, on which nuclei are formed) decreases basically in a short time (≈3 min) and then the exhaustion of the active centers is slower – see Fig. 15.

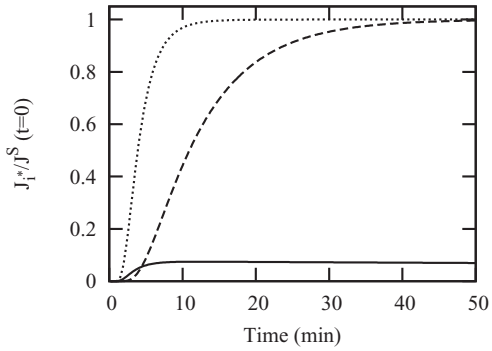

FIG. 13. Dimensionless nucleation rate, J_{i^*}/J^S, as a function of time. Solid and dotted lines correspond to the numerical solution of Eq. (6) with boundary conditions (16) and (17), dashed line to the analytical solution [see Eqs. (3)–(5)].

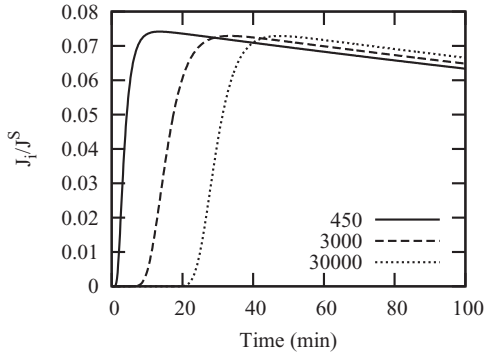

FIG. 14. Nucleation rate, J_i, normalized by the stationary nucleation rate, J^S, as a function of time for $i = 450$ (solid line), 3000 (dashed line), and 30 000 (dotted line).

D. Crystal nucleation from solution

Similarly as in, Kožíšek *et al.*[33] we have selected the two-component ideal solution with the following material parameters: $\sigma = 0.08\,\mathrm{J\,m^{-2}}$, the relative atomic masses of A, B components: $M_A = 18$, $M_B = 14$; the kinetic barrier of nucleation $E = 70\,000\,\mathrm{J\,mol^{-1}}$, temperature $T = 300\,\mathrm{K}$, the equilibrium concentration $C_0 = 0.1$, the densities of liquid components A, B: $\varrho_A^L = 1000\,\mathrm{kg\,m^{-3}}$, $\varrho_B^L = 900\,\mathrm{kg\,m^{-3}}$, and the density of the solid phase $\varrho_A^S = 1000\,\mathrm{kg\,m^{-3}}$.

The analytical approach to the total number of supercritical nuclei, Z_{i^*}, [see Eqs.(3)–(5), dashed line in Fig. 16] goes faster to the total number of active centers, N_{AC}, in comparison with the numerical solution using boundary condition (17) [solid line] for $\alpha = 90°$, $N_{AC} = 10^{18}\,\mathrm{m^{-3}}$, and initial supersaturation $C_i = 0.85$ – see Fig. 16. The number of supercritical nuclei, Z_{i^*}, increases with the initial supersaturation S_i – compare solid ($S_i = 0.85$), dotted ($S_i = 0.75$), and dot-and-dashed ($S_i = 0.60$) lines in Fig. 16. The kinetics of formation of nuclei is slower at higher nucleation barrier, i.e., at lower initial supersaturation.

The stationary nucleation rate decreases with time as supersaturation of solution decreases according to Eq. (18) and also the exhaustion of active centers occurs [see Eq. (17)].

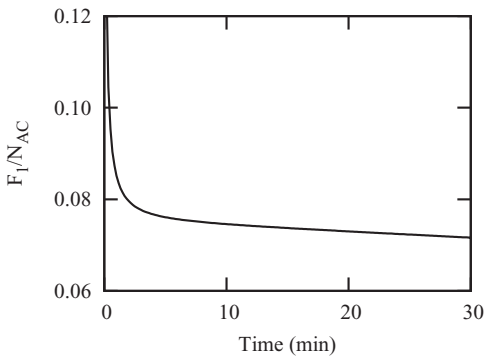

FIG. 15. Decrease of active centers, F_1 [see Eq. (17)], normalized by the total number of active centers, N_{AC}, as a function of time.

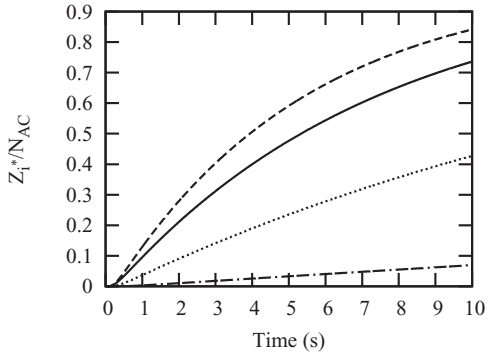

FIG. 16. The total number of supercritical nuclei per active center, Z_{i^*}/N_{AC}, as a function of time for $\alpha = 90^\circ$, $N_{AC} = 10^{18}\,\mathrm{m}^{-3}$, and the initial concentration $C_i = 0.85$ (solid line), 0.75 (dotted line), and 0.6 (dashed-and-dotted line). Dashed line corresponds to the analytical solution [Eqs. (3)–(5)] for $C_i = 0.85$.

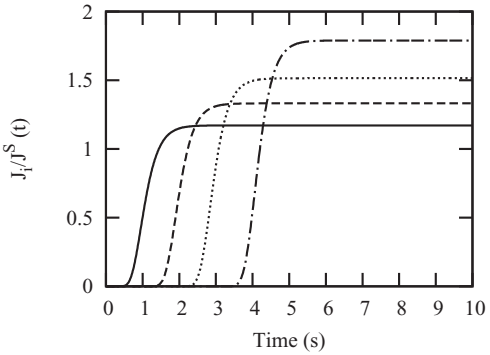

FIG. 18. Nucleation rate, J_i, normalized by the stationary nucleation rate (at corresponding time) as a function of time for $i = 50$ (solid line), 300 (dashed line), 1000 (dotted line), and 3000 (dot-and-dashed line).

Nucleation rate for nucleus sizes $i = 7$ ($\approx i^*$), 50, 300, 1000, and 3000 (solid lines from left to right in Fig. 17) reaches a maximum and then decreases with time – see Fig. 17. However, the analytical solution of the nucleation rate at the critical size [dashed line, Eq. (4)] reaches its stationary value (the number of active centers remains unchanged). The time delay of nucleation increases with nucleus size – see Fig. 17.

The nucleation rate normalized by its stationary value at a time t, $J_i/J^S(t)$, reaches a quasistationary value, which only slightly increases with time – see Fig. 18. This quasistationary limit and also the time delay of nucleation increase with nucleus size, i, – compare solid ($i = 50$), dashed ($i = 300$), dotted ($i = 1000$), and dot-and-dashed ($i = 3000$) lines in Fig. 18. After a time delay of nucleation, the quasistationary values $J_i/J^S(t) > 1$, i.e., the nucleation rate, $J_i(t)$, is higher than its stationary value $J^S(t)$ at the corresponding time t. The higher value of the quasistationary nucleation rate corresponds to some delay in nucleation kinetics, as the stationary nucleation rate, $J^S(t)$, decreases with time.

We have compared the temporal dependencies of the number of nuclei at size $i = 1000$ and $N_{AC} = 10^{18}\,\mathrm{m}^{-3}$ for various initial concentrations C_i, and wetting angles α – see Fig. 19. At $C_i = 0.85$, $\alpha = 90^\circ$ (solid line) the number of nuclei is higher than at $C_i = 0.85$, $\alpha = 110^\circ$ (dashed line) and $C_i = 0.6$, $\alpha = 90^\circ$ (dotted line). At $C_i = 0.85$, $\alpha = 90^\circ$ (solid line) the number of nuclei after reaching maximum decreases with time. At $C_i = 0.85$, $\alpha = 110^\circ$ (dashed line) and $C_i = 0.6$, $\alpha = 90^\circ$ (dotted line) the number of nuclei reaches approximately the same maximum, and decreases only slightly with time. The different behavior of the number density of nuclei in dependence of time is probably caused by the different nucleation barrier: $W^*/(k_B T) = 7.13$ at $C_i = 0.85$ and $\alpha = 90^\circ$; 10.65 at $C_i = 0.85$ and $\alpha = 110^\circ$; and 10.18 at $C_i = 0.6$ and $\alpha = 90^\circ$. Thus the similar course of the number of nuclei at $C_i = 0.85$, $\alpha = 100^\circ$ (dashed line), and $C_i = 0.6$, $\alpha = 90^\circ$ (dotted line) is the consequence of comparable nucleation barriers.

A decrease in supersaturation is very slow at initial supersaturation $S_i = 8.5$, $N_{AC} = 10^{18}\,\mathrm{m}^{-3}$, and $\alpha = 90^\circ$, but it is faster for lower wetting angle and higher number of the active centers. The influence of the wetting angle (see Fig. 4, crystal nucleation from vapor) and the number of active centers (see Fig. 11, formation of droplets from vapor) on supersaturation is similar as in previous considered systems.

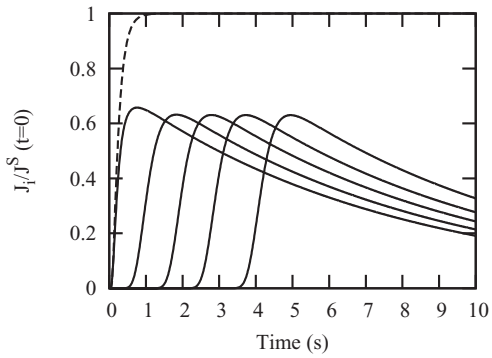

FIG. 17. Nucleation rate, J_i, normalized to the initial stationary nucleation rate (J^S at $t = 0$) as a function of time for $i = 7$, 50, 300, 1000, and 3000 (solid lines from left to right). The dashed line corresponds to the analytical solution of the nucleation rate [see Eq. (4)] at the critical size $i^* = 7$.

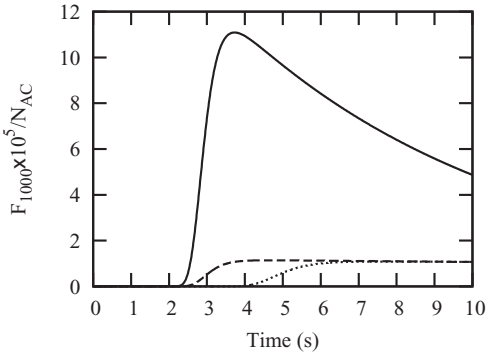

FIG. 19. The number of nuclei at size $i = 1000$ normalized by the total number of active centers, N_{AC}, as a function of time. Solid, dashed, and dotted lines correspond to $C_i = 0.85$ (initial concentration) and $\alpha = 90^\circ$, $C_i = 0.85$ and $\alpha = 110^\circ$, and $C_i = 0.60$ and $\alpha = 90^\circ$.

IV. CONCLUSIONS

We have introduced model of nucleation on active centers including decrease in supersaturation of the mother phase as a consequence of the phase transition. In a difference to the standard model of nucleation on active centers [which introduces Eq. (1) to include a depletion of active centers] the exhaustion of active centers is taken into account through the boundary condition – see Eq. (17). We have applied our model to crystal nucleation from supersaturated vapor, solution, supercooled melt, and also for formation of droplets in supersaturated vapor. In all systems under consideration the basic characteristics of nucleation (the number of nuclei, nucleation rate, exhaustion of active centers) exhibit a similar behavior in our model in dependence on the input parameters (temperature, supersaturation, interfacial energies). The total number of supercritical nuclei reaches the number of active centers faster in the standard model [i.e., exhaustion of active centers governed by Eq. (1) is faster] in comparison with our model. Exhaustion of active centers is faster at lower wetting angle (lower nucleation barrier). Nucleation rate (i.e., the time derivative of the number of supercritical nuclei) increases with time to some maximum and then decreases to zero as the number of supercritical nuclei reaches the total number of nuclei N_{AC}. The stationary nucleation rate, $J^S(t)$, at corresponding time t decreases with time as the exhaustion of active centers occurs. Nucleation rate reaches some quasistationary value higher than the stationary nucleation rate $J^S(t)$. Higher values of nucleation rate in comparison with $J^S(t)$ corresponds to the stationary nucleation rate at a shorter time. Standard model, based on nucleation rate derived at constant number of active centers, does not predict nucleation rate correctly (exhaustion of active centers is not reflected in nucleation rate). As the phase transformation occurs, part of molecules is "transferred" from the supersaturated (or supercooled) mother phase to the newly forming crystalline (or liquid) phase. This process influences the formation of nuclei (especially at higher number of active centers) of crystalline phase from supersaturated vapor and solution and also for droplet formation from supersaturated vapor, but does not influence the crystal nucleation of supercooled melt. The decrease in supersaturation of the mother phase is faster for higher number of the total number of active centers. Formation of nuclei is influenced by a decrease of supersaturation of the mother phase only at higher number of active centers, N_{AC} (N_{AC} limit, above which the decrease in supersaturation is evident, depends on the system under consideration).

ACKNOWLEDGMENTS

This work was supported by the (Grant No. IAA100100806) Grant Agency of the Academy of Sciences of the Czech Republic. Partial support from the Grant Agency of the Czech Republic (Grant Nos. P108/11/0937 and P108/12/0891) is gratefully acknowledged.

[1] K. F. Kelton and A. L. Greer, *Nucleation in Condensed Matter* (Elsevier, 2010), Vol. 15.
[2] D. Kashchiev, *Nucleation: Basic Theory with Applications* (Butterworth-Heinemann, An imprint of Elsevier Science, Linacre House, Oxford, 2000).
[3] H. Kumomi and F. G. Shi, Phys. Rev. Lett. **82**, 2717 (1999).
[4] V. M. Fokin, N. S. Yuritsin, V. N. Filipovich, and A. M. Kalinina, J. Non-Cryst. Solids **219**, 37 (1997).
[5] M. Hikosaka, S. Yamazaki, I. Wataoka, N. C. Das, K. Okada, A. Toda, and K. Inoue, J. Macromol. Sci. **42**, 847 (2003).
[6] K. Okada, K. Watanabe, T. Urushihara, A. Toda, and M. Hikosaka, Polymer **48**, 401 (2007).
[7] T. Urushihara, K. Okada, K. Watanabe, A. Toda, E. Tobita, N. Kawamoto, and M. Hikosaka, Polymer J. **39**, 55 (2007).
[8] R. B. McClurg, J. Chem. Phys. **59**, 5779 (2004).
[9] I. Markov and D. Kashchiev, J. Cryst. Growth **13**, 131 (1972).
[10] M. Avrami, J. Chem. Phys. **7**, 1103 (1939).
[11] M. Avrami, J. Chem. Phys. **8**, 212 (1940).
[12] Z. Kožíšek, P. Demo, and M. Nesladek, J. Chem. Phys. **108**, 9835 (1998).
[13] Z. Kožíšek, P. Demo, and K. Sato, J. Cryst. Growth **209**, 198 (2000).
[14] Z. Kožíšek, T. Koga, K. Sato, and P. Demo, J. Chem. Phys. **114**, 7622 (2001).
[15] Z. Kožíšek and P. Demo, J. Chem. Phys. **118**, 6411 (2003).
[16] Z. Kožíšek, M. Hikosaka, P. Demo, and A. M. Sveshnikov, J. Chem. Phys. **121**, 1587 (2004).
[17] Z. Kožíšek, M. Hikosaka, K. Okada, and P. Demo, J. Chem. Phys. **134**, 114904 (2011).
[18] F. F. Abraham, J. Chem. Phys. **51**, 1632 (1969).
[19] Z. Kožíšek, Czech. J. Phys. **40**, 592 (1990).
[20] Z. Kožíšek and P. Demo, J. Aerosol. Sci. **40**, 802 (2009).
[21] V. A. Shneidman, Sov. Phys.-Tech. Phys. **33**, 1338 (1988).
[22] W. G. Courtney, J. Chem. Phys. **35**, 2249 (1961).
[23] G. Wilemski and B. E. Wyslouzil, J. Chem. Phys. **103**, 1137 (1995).
[24] L. Zhou and H. Huang, e-print arXiv:1112.3278v1 [cond-mat.mtrl-sci].
[25] L. Schimka, J. Harl, A. Stroppa, A. Grüneis, M. Marsman, F. Mittendorfer, and G. Kresse, Nature Mater. **9**, 741 (2010).
[26] D. Turnbull and J. Fisher, J. Chem. Phys. **17**, 71 (1949).
[27] S. J. Cooper, C. E. Nicholson, and J. Liu, J. Chem. Phys. **129**, 124715 (2008).
[28] K. Okada, K. Watanabe, I. Wataoka, A. Toda, S. Sasaki, K. Inoue, and M. Hikosaka, Polymer **48**, 382 (2007).
[29] S. S. Kadam, H. J. M. Kramer, and J. H. ter Horst, Cryst. Growth Des. **11**, 1271 (2011).
[30] R. Grossier, Z. Hammadi, R. Morin, A. Magnaldo, and S. Veesler, Appl. Phys. Lett. **98**, 091916 (2011).
[31] R. Grossier, Z. Hammadi, R. Morin, and S. Veesler, Phys. Rev. Lett. **107**, 025504 (2011).
[32] D. Kashchiev, J. Chem. Phys. **134**, 196102 (2011).
[33] Z. Kožíšek, K. Sato, S. Ueno, and P. Demo, J. Chem. Phys. **134**, 094508 (2011).
[34] Z. Kožíšek and P. Demo, J. Chem. Phys. **123**, 144502(1) (2005).
[35] R. Strey and Y. Viisanen, J. Chem. Phys. **99**, 4693 (1993).